The Solution Structure of a Copper(II) Compound of a New Cyclic Octapeptide by EPR Spectroscopy and Force Field Calculations

Peter Comba,*,†,[1a] Rodney Cusack,[1b] David P. Fairlie,[1c] Lawrence R. Gahan,[1d] Graeme R. Hanson,[1b] Uli Kazmaier,[1e] and Anne Ramlow[1a]

Anorganisch-Chemisches and Organisch-Chemisches Institut der Universität, Im Neuenheimer Feld 270, D-69120 Heidelberg, Germany, and Department of Chemistry, Centre for Magnetic Resonance, and 3D Centre, The University of Queensland, Brisbane, QLD, 4072 Australia

Received August 5, 1998

A new cyclic octapeptide, cyclo(Ile-Ser-(Gly)Thz-Ile-Thr-(Gly)Thz) (PatN), related to patellamide A, has been synthesized and reacted with copper(II) and base to form mono- and dinuclear complexes. The coordination environments around copper(II) have been characterized by EPR spectroscopy. The solution structure of the thermodynamically most stable product, a purple dicopper(II) compound, has been examined by simulating weakly dipole−dipole coupled EPR spectra based upon structural parameters obtained from force field (MM and MD) calculations. The MM−EPR method produces a saddle-shaped structure for $[Cu_2(PatN)(OH_2)_6]$ that is similar to the known solution structure of patellamide A and the known solid-state structure of $[Cu_2(AscidH_2)CO_3(OH_2)_2]$. Compared with the latter, $[Cu_2(PatN)]$ has no carbonate bridge and a significantly flatter topology. The MM−EPR approach to solution-structure determination for paramagnetic metallopeptides may find wide applications to other metallopeptides and metalloproteins.

Introduction

Because of their specific chemical and biological properties, novel cyclic peptides containing unusual amino acids, isolated from bacteria, fungi, and marine organisms, have recently attracted much attention.[2] The absence of C- and N-termini leads to hydrolytic stability, which makes these cyclic peptides important for pharmaceutical applications. Certain cyclic peptides have been found to be efficient enzyme inhibitors and immunoregulators and to have antibiotic, antineoplastic, and/or antiinflammatory activity.[2,3] The capacity of some marine organisms to accumulate various metal ions has been related to the presence of cyclic peptides[2a,4] (*Lissoclinum patella*, e.g., concentrates copper(II) by a factor of 10^4 with respect to its environment). There is little evidence to date for the direct involvement of the secondary metabolites, and metal ion selective complexation has been demonstrated by circular dichroism.[4]

Only a few metal complexes of cyclic peptides have been structurally characterized.[2a,5] Of particular interest for an understanding of biological activities are solution structural properties. NMR techniques in combination with force field calculations (MM and MD) have been used to study the solution structures of metal-free cyclic peptides.[6] Our recently developed technique to predict and determine solution structures of dicopper(II) compounds, based on force field calculations and the simulation of weakly dipole−dipole coupled EPR spectra (MM−EPR[7]), was thought to be an ideal tool to study the corresponding dicopper(II) compounds. For a systematic investigation of complexation and structural properties, a variety of derivatives of metal-free ligands need to be available in reasonable quantity. Procedures for the synthesis of thiazole-containing cyclic peptides of this type have been developed to some extent,[8] but reports of metal complexes of synthetic cyclic peptides of this type are rare.

† Telefax: Int. +6221/546617. E-mail: comba@akcomba.oci.uni-heidelberg.de.

(1) (a) Anorganisch-Chemisches Institut, Universität Heidelberg; (b) Centre for Magnetic Resonance, The University of Queensland; (c) 3D Centre, The University of Queensland; (d) Department of Chemistry, The University of Queensland; (e) Organisch-Chemisches Institut, Universität Heidelberg.

(2) (a) Michael, J. P.; Pattenden, G. *Angew. Chem. Int. Ed. Engl.* **1993**, *105*, 1. (b) Lewis, J. R. *Nat. Prod. Rep.* **1989**, *6*, 503. (c) Faulkner, D. J. *Nat. Prod. Rep.* **1988**, *5*, 613. (d) Krebs, H. C. *Fortschr. Chem. Org. Naturst.* **1986**, *49*, 151. (e) Fairlie, D. P.; Abbenante, G.; March, D. M. *Curr. Med. Chem.* **1995**, *2*, 672.

(3) (a) Rosen, M. K.; Schreiber, S. L. *Angew. Chem., Int. Ed. Engl.* **1992**, *31*, 384. (b) Evans, D. A.; Ellman, J. A. *J. Am. Chem. Soc.* **1991**, *11*, 1063. (c) Fusetani, N.; Sugawara, T.; Matsunaga, S. *J. Am. Chem. Soc.* **1991**, *113*, 7811.

(4) (a) van den Brenk, A. L.; Ph.D. Thesis, University of Queensland, **1994**; (b) Freeman, D. J.; Pattenden, G.; Drake, A. F.; Siligardi, G. *J. Chem. Soc., Perkin Trans. 2* **1998**, 129−135.

(5) (a) van den Brenk, A. L.; Fairlie, D. P.; Gahan, L. R.; Hanson, G. R.; Hawkins, C. J.; Jones, A. *Inorg. Chem.* **1994**, *33*, 2280. (b) van den Brenk, A. L.; Byriel, K. A.; Fairlie, D. P.; Gahan, L. R.; Hanson, G. R.; Hawkins, C. J.; Jones, A.; Kennard, C. H.; Moubaraki, B.; Murray, K. S. *Inorg. Chem.* **1994**, *33*, 3549. (c) van den Brenk, A. L.; Fairlie, D. P.; Gahan, L. R.; Hanson, G. R.; Hambley, T. W. *Inorg. Chem.* **1996**, *35*, 1095. (d) Abbenante, G.; Fairlie, D. P.; Gahan, L. R.; Hanson, G. R.; Pierens, G. *J. Am. Chem. Soc.* **1996**, *118*, 10384.

(6) (a) Ishida, T.; Tanaka, M.; Nabae, M.; Inoue, M.; Kato, S.; Hamada, Y.; Shioiri, T. *J. Org. Chem.* **1988**, *53*, 107. (b) Ishida, T.; In, Y.; Shinozaki, F.; Doi, M.; Yamamoto, D.; Hamada, Y.; Shioiri, T.; Kamigauchi, M.; Sugiwra, M. *J. Org. Chem.* **1995**, *60*, 3944. (c) Foster, M. P.; Concepcion, G. P.; Caraan, G. B.; Ireland, C. M. *J. Org. Chem.* **1992**, *57*, 6671. (d) White, J. D.; Chong, W. K. M.; Thirring, K. *J. Org. Chem.* **1983**, *48*, 2302. (e) Morita, H.; Yoshida, N.; Takeya, K.; Itokawa, H.; Shirota, O. *Tetrahedron* **1996**, *52*, 2795. (f) Schmitz, F. J.; Ksebati, M. B.; Chang, J. S.; Wang, J. L.; Hossain, M. B.; van der Helm, D. *J. Org. Chem.* **1989**, *54*, 3463.

(7) (a) Bernhardt, P. V.; Comba, P.; Hambley, T. W.; Massoud, S. S.; Stebler, S. *Inorg. Chem.* **1992**, *31*, 2644. (b) Comba, P. *Comments Inorg. Chem.* **1994**, *16*, 133. (c) Comba, P.; Hambley, T. W.; Hilfenhaus, P.; Richens, D. T. *J. Chem. Soc., Dalton Trans.* **1996**, 533, (d) Comba, P.; Hilfenhaus, P. *J. Chem. Soc., Dalton Trans.* **1995**, 3269.

10.1021/ic9809299 CCC: $15.00
Published on Web 12/03/1998

Chart 1

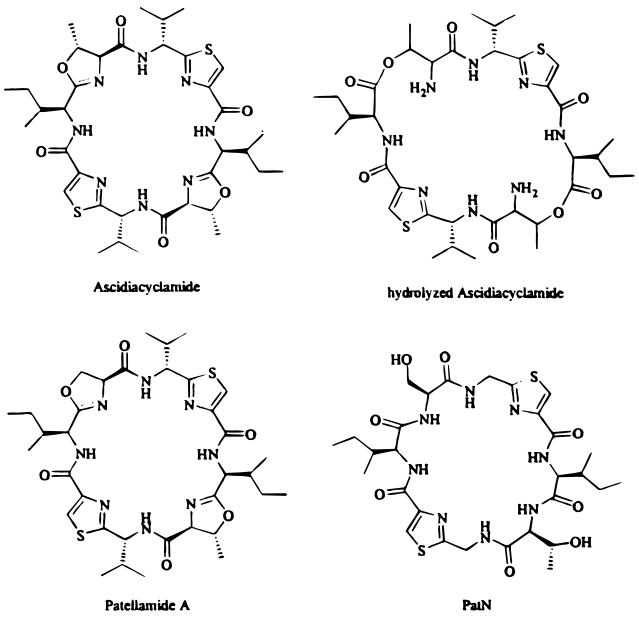

We have focused on a synthetic patellamide A derivative, cyclo(Ile-Ser-(Gly)Thz-Ile-Thr-(Gly)Thz) (PatN), because of its relative simplicity and its similarity with patellamides (see Chart 1). The main difference between PatN and patellamide A is the open oxazoline rings which increase the flexibility of the ligand backbone. Similar structural features have been observed in hydrolyzed ascidiacyclamide (see Chart 1), for which the crystal structural analysis of a potassium complex was reported.[5c,d] The substitution of one Thr by Ser, in comparison to ascidiacyclamide, leads to asymmetry which was expected to simplify the NMR-spectroscopic analysis without leading to significant distortion of the saddle-shaped conformation observed for symmetric patellamides. Val was substituted by Gly, in comparison to patellamide A, to eliminate possible epimerization of the asymmetric center α to the thiazole ring.[9] We report the synthesis and characterization of the new cyclic octapeptide, its mono- and dicopper(II) compounds, and the solution-structure determination of $[Cu_2(PatN)(OH_2)_6]$.

Results and Discussion

Synthesis of PatN. A synthetic procedure[24] for PatN is shown in Scheme 1. A variety of coupling reagents were tested for each reaction:[10] DPPA was used for the coupling of the dipeptides, TBTU led to the best results for the tetrapeptides, the best yields for the linear octapeptide were obtained with ethylchloroformate, and the cyclization was performed with HATU. The hydrolysis of the esters of the tetrapeptides was not as straightforward as expected. Reaction with NaOH, LiOH in tetrahydrofuran, and LiOH in combination with *tert*-butylmercaptan and ethanethiol did not result in any hydrolysis. Therefore, the corresponding methyl ester was prepared by a known method,[11] and this was hydrolyzed with LiOH in tetrahydrofuran. The methyl ester of the linear octapeptide was hydrolyzed with NaOH in DMF.

Scheme 1

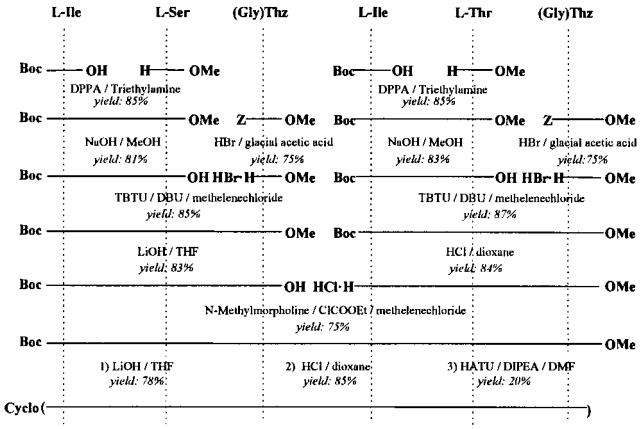

The cyclized product, PatN, was purified by RP-HPLC, followed by freeze-drying. It was characterized by analytical reverse phase HPLC, high-resolution mass spectroscopy, two-dimensional ^{1}H NMR spectroscopy, UV−vis, and CD spectroscopy.

The UV−vis and CD spectra ($\pi \rightarrow \pi^*$ (thiazole rings) at 220 nm; n $\rightarrow \pi^*$ (conjugated thiazole/carbonyl fragments) at 320 nm; and positive Cotton effect at 275 nm (for details see the Experimental Section) are consistent with the proposed structure, and the MS (ion-spray) signal at *m*/*z* 695.2 $[M + H]^+$ and HRMS (FAB+) signals at $m/z = 695.2652$, $[M + H]^+$ calculated for $C_{29}H_{43}N_8O_8S_2$ 695.2566, and $m/z = 694.2548$, M^+ calculated for $C_{29}H_{42}N_8O_8S_2$ 694.2566, confirm the composition of PatN. The ^{1}H NMR (d_3-methanol) chemical shifts and the coupling constants (assignment of the resonances by 2D TOCSY and COSY analyses) are in agreement with the expected structure of PatN (see Table 1).

^{1}H NMR spectra in d_4-methanol show slow exchange behavior (90 min) for the Gly amide protons which indicates a degree of protection from the solvent that is indicative of intramolecular hydrogen bonding. Also included in Table 1 are the temperature-dependent chemical shifts of the amide protons. The small shifts with temperature (<1−2 ppb/deg) of the Gly amide protons confirm their involvement in H-bonding.[12a] The $^3J_{NH-\alpha H}$ coupling constants for the amide NH protons (Table 1) differ from the conformationally averaged value of 6−7 Hz[12b] for the Gly residues, supporting their involvement in hydrogen bonds. Unfortunately, there were insufficient transannular NOEs to permit a structure calculation.

Mononuclear Copper(II) Compounds. Investigation of the copper(II) coordination chemistry of ascidiacyclamide and patellamide D indicated that various mononuclear species are present. These were characterized spectroscopically,[5] but no crystal structures have been reported so far.

Blue solutions of the mononuclear copper(II) compounds of PatN were obtained by addition of 1 equiv of copper(II) in methanol (chloride or nitrate salt) to a 2 mM solution of PatN in methanol (the peptide content of the PatN solution was determined by titration with copper(II), see the Experimental Section),

(8) (a) Wipf, P.; Venkatraman, S.; Miller, C. P.; Geib, S. J. *Angew. Chem., Int. Ed. Engl.* **1994**, *33*, 1516−1518; Wipf, P. *Chem. Rev.* **1995**, *95*, 2115 and references cited within.

(9) (a) Wipf, P.; Fritsch, P. *Tetrahedron Lett.* **1994**, *35*, 5397. (b) Wipf, P.; Miller, C.; *Tetrahedron Lett.* **1992**, *33*, 907. (c) Wipf, P.; Miller, C. *J. Org. Chem.* **1993**, *58*, 1575.

(10) (a) Knorr, R.; Trzeciak, A.; Bannwarth, W.; Gillessen, D. *Tetrahedron Lett.* **1989**, *30*, 1927. (b) Carpino, L. A.; El-Faham, A.; Minor, C. A.; Alberico, F. *J. Chem. Soc., Chem. Commun.* **1994**, 201. (c) Ehrlich, A.; Rothemund, S.; Brudel, M.; Beyermann, M.; Carpino, L. A.; Bienert, M. *Tetrahedron Lett.* **1993**, *34*, 4781.

(11) Seebach, D.; Thaler, A.; Blaser, D.; Ko, S. Y. *Helv. Chim. Acta* **1981**, *74*, 1102.

(12) (a) Kessler, H. *Angew. Chem. Int. Ed. Engl.* **1982**, *21*, 512. (b) Dyson, H. J.; Wright, P. E. *Annu. Rev. Biophys. Biophys. Chem.* **1991**, *20*, 519−538.

Table 1. ^{1}H NMR Data for PatN in d_3-Methanol

	Ile(1)	Ser(2)	Gly(3)	Ile(4)	Thr(5)	Gly(6)
NH	9.15	8.92	8.15	9.50	9.60	8.25
αH	4.15	4.47	4.30, 4.31	4.19	3.97	5.20, 5.14
βH	2.40	3.98, 3.89		2.50	4.64	
γH	1.70, 1.17, 0.99 (CH_3)			1.80, 1.20, 1.07 (CH_3)	1.26	
δH	0.90			0.91		
	Amide−NH Proton Coupling Constants in d_4-Methanol					
$^3J_{NH-\alpha CH}$ (Hz)	6.80	7.04	8.33, 1.89	6.49	6.80	9.52, 1.89
	Variable Temperature Data, Calculated over a 20 °C Range					
$\Delta\delta/T$ (ppb/K)	5.0[a]	8.5	1.0	5.0	12.0[a]	2.0

[a] Peaks merged and therefore ppb/°C was calculated over 10 °C.

followed by the slow addition of base (1 or 2 equiv, triethylamine solution in methanol). The UV−vis and CD spectra of these solutions are independent of the copper(II) salt used, indicating that, for PatN, there is no coordination of chloride in the mononuclear complexes. The mononuclear complexes convert slowly to the dinuclear species (see below) and free ligand, and this process is accelerated in base. Therefore, samples of the mononuclear species were frozen directly after their preparation to ensure identical samples for all spectroscopic measurements.

MS (ion-spray) spectra indicate the presence of $[Cu(H_5PatN)]^+$ together with the protonated peptide, its adduct with triethylamine, and dinuclear compounds (PatN has six amide protons (see Chart 1); therefore, in cases where the degree of protonation is evident and of importance, it will be indicated in the formulas, i.e., the fully protonated form is H_6PatN, and $[Cu(H_5PatN)]^+$ is the copper(II) compound of the monodeprotonated ligand). The presence of dinuclear species and free peptide indicates the relative instability of the mononuclear complexes. The instability of solutions of the metal complex toward formation of the dinuclear compound did not allow an unambiguous analysis of the spectra in terms of the equivalents of added base (for a full analysis of the MS spectra see the Experimental Section).

The spectrophotometric titration of 1:1 mixtures of copper(II) and PatN with triethylamine in methanol indicates that two different species are present, with one or two deprotonated amides, respectively. Both give strong LMCT transitions in the UV region. After the addition of 1 equiv of base, a copper(II) d−d transition appears at 708 nm ($\epsilon \sim 40$ M^{-1} cm^{-1}), and this shifts to higher energy upon addition of a second equivalent of base (585 nm, $\epsilon \sim 90$ M^{-1} cm^{-1}). The latter transition is consistent with the coordination of two deprotonated amide nitrogens and probably one or two further nitrogen donors provided by the thiazole rings. The shift to lower energy, when only 1 equiv of base is added, is consistent with a chromophore that involves mainly oxygen donors in addition to the one deprotonated amide, and a donor set similar to that observed in the potassium complex of the hydrolyzed ascidiacyclamide is consistent with these observations.[5]

Multifrequency EPR spectroscopy (S-, Q-, and X-bands) at 298 and 130 K of 1:1:1 and 1:1:2 (Cu^{2+}/PatN/base) solutions was used to determine the spin Hamiltonian parameters of the mononuclear copper(II) complexes of PatN. The spectroscopic features of the dinuclear compounds (see below) were subtracted from the experimental spectra, and all spectra could then be simulated[13] assuming three axially symmetric species (Table 2), i.e., three significantly different mononuclear [Cu(PatN)] compounds are observed. The spectra of all the mononuclear copper(II) complexes are obtained after addition of only 1 equiv of base and indicate an approximate ratio of the three mononuclear species of 10:63:27, i.e., $[Cu(H_4PatN)]$ is the major species. All spectra obtained for a Cu^{2+}/PatN/base ratio of 1:1:2 indicate that $[Cu(H_4PatN)]$ is obtained almost exclusively.

Table 2. *g*- and *A*-Values and Line Widths of the Mononuclear Copper(II) Species and Free Copper in Methanol[a]

complex	$g_\parallel$	$g_\perp$	$A_\parallel$	$A_\perp$	$\sigma_\parallel$	$\sigma_\perp$
$[Cu(MeOH)_n]^{2+}$	2.4235	2.0884	119.51	3.32	35	15
$[CuH_4PatN]$	2.2154	2.0505	180.00	5.50	30	60
$[CuH_5PatN]^+$	2.4200	2.0750	127.00	2.00	35	25
unidentified species	2.2800	2.0900	145.00	2.00	35	40

[a] *A*-values and line widths are given in 10^{-4} cm^{-1}.

The two major species, $[Cu(H_5PatN)]^+$ (mono-deprotonated PatN) and $[Cu(H_4PatN)]$ (bis-deprotonated PatN), differ considerably in their spin Hamiltonian parameters. The former has a large $g_\parallel$ and a small $A_\parallel$ value, similar to those observed for free copper(II) in methanolic solution (Table 2). Indeed, Blumberg−Peisach plots[14] indicate that the copper(II) ion in $[Cu(H_5PatN)]^+$ is primarily coordinated to oxygen donors. This is in good agreement with the interpretations based on the electronic spectra (see above). The relatively small $g_\parallel$ and large $A_\parallel$ values of $[Cu(H_4PatN)]$ indicate a relatively strong in-plane ligand field, i.e., relatively strong donors and little distortion from planarity in the *xy* plane.[15] This might indicate that at least one thiazole nitrogen is coordinated in addition to the two deprotonated amide donors.

Dinuclear Copper(II) Compounds. The dicopper(II) compounds of ascidiacyclamide and patellamide D have been studied extensively.[5] Various dinuclear species, including hydroxo and carbonato complexes, were identified by ion-spray mass spectroscopy, the relative orientations of the *g*-matrixes were analyzed by EPR spectroscopy in solution, and an X-ray crystal structural analysis of $[Cu_2(AscidH_2)(\mu^2\text{-}CO_3)(OH_2)_2]$ ($AscidH_4$ = ascidiacyclamide) was reported.[5] The saddle-shaped conformation is retained in the dicopper(II) compound, and the two five-coordinate copper(II) centers are each coordinated to three nitrogen donors (oxazoline, thiazole, and *N*-amide from Ile) and two oxygens (one water and the μ-1,2 bridging carbonate). Solution studies (primarily EPR) of this compound indicate that, in methanol, there is a structural rearrangement. That is, the structure of $[Cu_2(AscidH_2)]$ in solution is different from that in the solid.

Addition of 2 equiv of a copper(II) salt (chloride or nitrate) in methanol to a solution (methanol) of 1 equiv of PatN, followed by the slow addition of four equivalents of base (NaOH in methanol) produces a blue solution of the dinuclear complexes. Addition of an additional 1 equiv of NaOH leads to a

(13) (a) Wang D.; Hanson, G. R. *Appl. Magn. Reson.* **1996**, *11*, 401, (b) Wang D.; Hanson, G. R. *J. Magn. Reson. Ser. A* **1995**, *117*, 1.

(14) Peisach, J.; Blumberg, W. E. *Arch. Biochem. Biophys.* **1974**, *165*, 691.

(15) Comba, P.; Hambley, T. W.; Hitchman, M. A.; Stratemeier, H. *Inorg. Chem.* **1995**, *34*, 3903.

color change from blue to purple. This color change (within less than 2 min) is not observed when the weaker base triethylamine is used instead of NaOH, but upon exposure to air, the former solution slowly changes to the same purple final product (within ca. 1 day). Further addition of base (up to 8 equiv, NaOH or triethylamine) does not lead to any further change. From EPR spectra of solutions of the blue and purple compounds and ion-spray mass spectra, it emerges that both are due to dicopper(II) compounds with distinctly different EPR, CD, and UV−vis spectra (see below). The analysis of the electronic spectra indicates that a linkage isomerization of the thiazole donor (N/S) is most unlikely.

As a result of the observation that in solution under basic conditions both patellamide D and ascidiacyclamide form carbonato-bridged dicopper(II) compounds, the possibility of carbonate coordination to the blue form of $[Cu_2(PatN)]$ was investigated in detail. Addition of sodium carbonate to the initial blue solution indeed leads to a change to the purple form. However, no mass spectroscopy evidence for coordinated carbonate was obtained employing ^{13}C-labeled carbonate in these experiments. Also, the complexation in degassed solutions in a rigorously air-free atmosphere leads to the same blue/purple transformation when a fifth equivalent of NaOH is added.

It became evident that the coordination of OH^- might be responsible for the color change. This idea is consistent with the mass spectroscopic observations (see the Experimental Section). Further support for this interpretation is based on IR spectroscopy. Bridging hydroxo groups are expected to have transitions in the region of 950 cm^{-1} that shift to around 750 cm^{-1} upon deuteration.[16] The complexity of the IR spectra of the dinuclear copper(II) compounds precludes an unambiguous interpretation, but the fact that the expected shifts could not be observed and that little difference between the spectra of natural abundance and deuterated samples in that region is seen indicates that the two copper(II) centers are probably not bridged by a hydroxide. More importantly, upon deuteration, there is a shift of a transition in the spectral region where M−OH resonances are expected, i.e., from 1400 to 1263 cm^{-1}.

The electronic spectra of the blue and purple dicopper(II) compounds have transitions at 590 and 540 nm, respectively (significant changes are also observed in the corresponding CD spectra, see the Experimental Section). It is unlikely that this shift to higher energy is due to a deprotonation of a coordinated water molecule: (i) the color change should then be immediate; the rate (1−2 min) indicates that some rearrangement process is involved; (ii) due to π donation, hydroxide leads, in contrast to the observation, to a decrease of the ligand field strength. Thus, the coordination of hydroxide probably leads to a change in coordination number and/or geometry. An increase in the electronic transition energy of the same order of magnitude has been observed and quantitatively analyzed in copper(II) complexes with four amine donors and an axially coordinated water molecule.[17] A shift of 30 nm toward higher energy was attributed to a twist along the Berry rotation coordinate toward square pyramidal geometry. As a consequence of the holohedral symmetry principles, a qualitatively similar effect may be expected along a rearrangement from distorted trigonal bipyramidal to distorted octahedral coordination geometry.

The absence of isosbestic points in a titration of a solution of Cu^{2+}/PatN, 2:1, with base in the UV−vis and CD spectra indicates that various species, are present. EPR spectra of the dinuclear complexes confirm this interpretation: the spectrum of the blue solution is a combination of the spectra of at least two species but that of the purple solution may be interpreted as a spectrum of a single weakly dipole−dipole coupled dicopper(II) compound. This is consistent with the observation that 1:1 as well as 2:1 (Cu^{2+}/PatN) solutions slowly lead to the same purple product in the presence of base, i.e., this is the thermodynamically most stable complex. The EPR spectra of this species were simulated,[18] and the results are presented in Table 3 and Figure 1.

Table 3. EPR Parameters of the Purple Dinuclear Copper(II) Complex[a]

$g_{\|\|}$	2.260	ξ [deg]	88
$g_\perp$	2.085	η [deg]	25
$A_{\|\|}$ [10^4 cm^{-1}]	82	τ [deg]	35
$A_\perp$ [10^4 cm^{-1}]	77	r_{Cu-Cu} [Å]	5.89
$\sigma_{\|\|}$ [MHz]	89		
$\sigma_\perp$ [MHz]	82		

[a] The structural parameters are given in Figure 2.

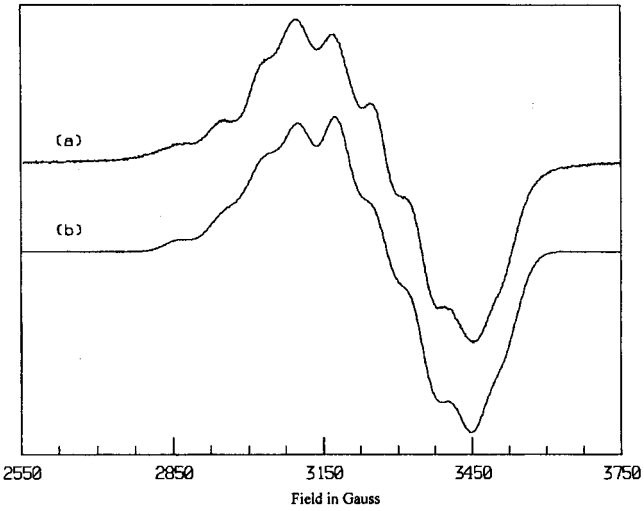

Figure 1. (a) Experimental X-band EPR spectrum of the purple dinuclear copper(II) complex at ν = 9.594 GHz; (b) the computer simulation of spectrum a.

The experimentally observed and simulated spectra are virtually superimposable. The $g_{\|\|}$ and $A_{\|\|}$ values indicate that there is a considerable distortion of the in-plane ligand field (see corresponding section of the mononuclear complexes above; note that *g*-values of dinuclear compounds are expected to be similar to those of corresponding mononuclear species, while the effective *A*-values, depending on the spin exchange rate between the two coordination centers, are generally smaller, with a limiting value of 50% of that observed for the corresponding mononuclear centers). The geometric parameters suggest a saddle-shaped conformation with a tilt angle involving the *z*-axes of the two **g**-tensors of 35°. The copper···copper distance of 5.89 Å is considerably smaller than that calculated for the dicopper(II) complex $[Cu_2(PatH_2)]^{2+}$ of patellamide D (6.8 Å) but larger than the crystallographically determined value reported for the dicopper(II) compound of ascidiacyclamide (4.43 Å). The latter value for the carbonato-bridged species indicates that the copper···copper separation observed here is too large for a bridged dinuclear compound, which is in agreement with the analysis based on MS and IR spectroscopy (see above). The decrease in the copper···copper distance in

(16) (a) Nakamoto, K. *Infrared and Raman Spectra of Inorganic and Coordination Compounds*, 4th ed.; John Wiley & Sons: New York, 1986. (b) Ferraro, J. R.; Walker, W. R. *Inorg. Chem.* **1965**, *4*, 1382. (c) McWhinnie, W. R. *J. Inorg. Nucl. Chem.* **1965**, *27*, 1063.
(17) Comba, P.; Hilfenhaus, P.; Nuber, B. *Helv. Chim. Acta* **1997**, *80*, 1831.
(18) Smith, T. D.; Pilbrow, J. R. *Coord. Chem. Rev.* **1974**, *13*, 173.

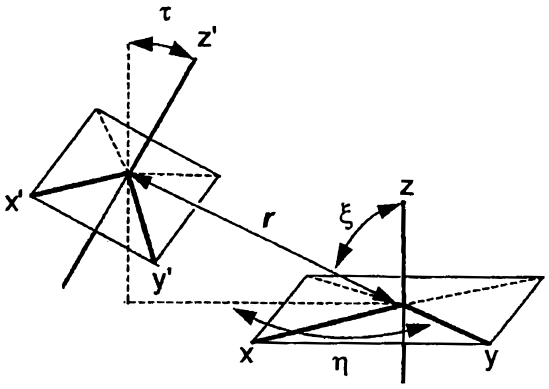

Figure 2. Definition of the angles ξ, τ, and η.

Table 4. Angles, Cu−Cu Distances, and Strain Energies of the Calculated Structures Compared with the Parameters from the EPR Simulation of the Purple Dinuclear Copper(II) Complex

	ξ [deg]	τ [deg]	η [deg]	r_{Cu-Cu} [Å]	strain energy [kJ/mol]
PatN1	75	31	26	5.28	86.0
PatN2	71	34	20	5.42	94.8
PatN3	43	2	17	4.96	125.8
EPR simulation	88	35	25	5.98	

comparison with the corresponding complex of patellamide D confirms the expectation that the open oxazoline rings lead to a more flexible ligand backbone.

Solution Structure of [Cu2(PatN)]. Molecular graphics was used to build a model of $[Cu_2(PatNH_2)]$, with the thiazole, two deprotonated amide nitrogen donors (Ile and Gly), and three water molecules coordinated to each of the copper(II) centers, based on the structural parameters of the EPR simulation of the purple solution (Table 3). Molecular dynamics was used for scanning the conformational space, and the structures of the local minima were optimized with force field calculations, using a program[19] and force field[20] that have been developed specifically for transition metal compounds (an extension of the force field is described in the Experimental Section). The structural parameters and strain energies of the three most favorable structures of $[Cu_2(PatNH_2)(OH_2)_3]$ (PatN1, PatN2, and PatN3) are given in Table 4, and plots of the structures are presented in Figure 3.

It is not unexpected that there are significant differences between the structural parameters obtained from the simulation of the observed EPR spectrum (also given in Table 4) and those obtained from the computed structures. These are due to (i) the fact that the axes of the **g**-tensors are similar but not identical to the axes of the internal coordinate systems of the chromophores (which are also not unambiguously assigned in distorted chromophores such as those of the computed structures here); (ii) remaining inconsistencies of the force field used; and (iii) the neglect of solvation in the computation of the structures.[7] The structure that is, on average, in best agreement with the parameters obtained from the EPR simulation is that of PatN1, and this also is the lowest strain energy structure. Model calculations (EPR simulations in dependence of specifically varied structural parameters) indicate that the shape of the spectrum

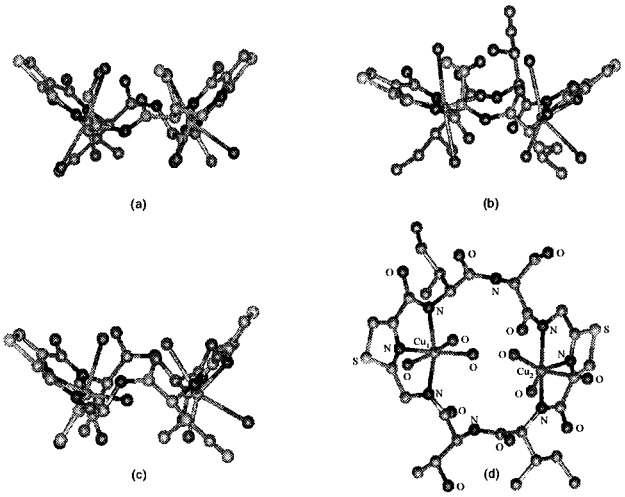

Figure 3. (a) PatN2, side view; (b) PatN3, side view; (c) PatN1, side view; (d) PatN1, top view.

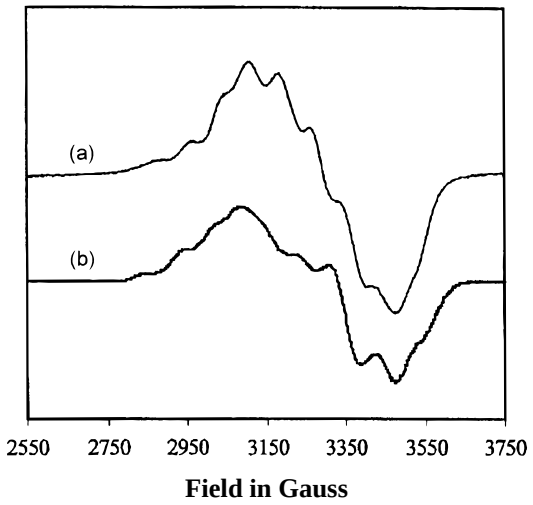

Figure 4. (a) Experimental X-band EPR spectrum of the purple dinuclear copper(II) complex; (b) simulated spectrum based on PatN1.

is mainly dependent on ξ (Figure 2); small variations of η and τ (up to 5°) and r_{Cu-Cu} (up to 0.5 Å) have only a minor influence on the peak positions and shapes. This also indicates that PatN1 is the most probable structure.

The simulated spectrum, based on PatN1, is compared to the experimental spectrum in Figure 4 (the simulation of a weighted average of the spectra of PatN1, PatN2, and PatN3 is not warranted because of uncertainties regarding the relative strain energies (neglected environmental effects) and because the energy difference between the global energy minimum and the other two structures indicates only a minor contribution of the less favorable species). There is acceptable agreement between the two spectra; the main difference is in the relative intensities, and these are not accurately computed because of *g*- and *A*-strain which are not included in the program, DISSIM, used here. The good agreement between the structural parameters obtained from the EPR simulation and those from molecular modeling further supports the assumption of two six-coordinate copper(II) centers with three nitrogen donors from the peptide and three oxygen donors from solvent molecules.

Conclusions

The successful synthesis and characterization of a new cyclic octapeptide and its mono- and dinuclear copper(II) compounds

(19) Comba, P.; Hambley, T. W.; Lauer, G.; Okon, N. *MOMEC97, A Molecular Modeling Package for Inorganic Compounds*; Lauer & Okon: Heidelberg, Germany, 1997; e-mail; CVS-HD@T-Online.de.

(20) (a) Bol, J. E.; Buning, C.; Comba, P.; Reedijk, J.; Ströhle, M. *J. Comput. Chem.* **1998**, *19*, 512. (b) Bernhardt, P. V.; Comba, P. *Inorg. Chem.* **1992**, *31*, 2368. (c) Comba, P.; Hambley, T. W.; Ströhle, M. *Helv. Chim. Acta* **1995**, *61*, 2042.

permitted the determination of the first solution structure of a dinuclear copper(II) complex of a synthetic octapeptide by MM−EPR. The geometric parameters, determined by the simulation of the EPR spectrum of the dinuclear complex, suggest a saddle-shaped conformation with a tilt angle of approximately 35°, which is less than that of known carbonate-bridged species of other peptides. This can be explained by the increased flexibility of the ligand backbone, due to open oxazoline rings. The synthesis and characterization of further modified patellamides may be helpful in understanding the conformational effects of structural constraints. Our work has been a step in this direction, and it is hoped that this will bring us closer to understanding the biological function of such molecules in Nature.

Experimental Section

Abbreviations. TFA = trifluoroacetic acid; DIPEA = diisopropylethylamine; HATU = *O*-(7-azabenzotriazol-1-yl)-1,1,3,3-tetramethyluronium hexafluorophosphate; DMF = dimethylformamide; Thz = thiazole; TBTU = 2-(1-hydroxy-1,2,3-benzotriazol-1-yl)-1,1,3,3-tetramethyluronium tetrafluoroborate; BOC = *tert*-butyloxycarbonyl; Z = benzyloxycarbonyl; THF = tetrahydrofuran; DPPA = diphenylphosphorazidate; DBU = 1,8-diazabicyclo[5.4.0]undec-7-ene; CD = circular dichroism; d = doublet; s = singlet; m = multiplet.

General Methods. Materials obtained commercially were reagent grade unless otherwise stated. ^{1}H NMR and ^{13}C NMR spectra were recorded on the following instruments: Bruker AMX 400 at 400 MHz (two-dimensional COSY and TOCSY spectra: 1 mg in 500 μL deuterated methanol, mixing time 75 ms, acquisition time 0.0116 s; referenced to solvent at 24 °C, recorded in the phase-sensitive mode, data were zero-filled and Fourier transformed to 1024 real points in both dimensions); Bruker WH 300 at 300 and 75.47 MHz; and Bruker AS 200 at 200 and 50.32 MHz. Preparative scale reverse phase *HPLC* separations were performed on Waters Delta-Pak PrepPak C_{18} 40 mm × 100 mm cartridges (100 Å) using gradient mixtures of water/0.1% TFA and 10% water/90% acetonitrile/0.1% TFA. Analytical reverse phase HPLC was performed on Waters Delta-Pak Radial-Pak C_{18} 8 mm × 100 mm cartridges (100 Å) using gradient mixtures of water/0.1% TFA and 10% water/90% acetonitrile/0.1% TFA.

IR spectra of KBr pellets were recorded with a Perkin-Elmer 16 PC FT instrument. A Beckman DU 75000 spectrometer was used to measure UV−vis spectra of 10^{-3}−10^{-6} M solutions in 1 or 0.1 cm quartz cells. CD spectra were recorded using a JASCO J-710 spectropolarimeter (N_2 flow of 4 L/min; 10^{-2}−10^{-4} M solutions; 1 or 0.1 cm quartz cells). The absorptions were recorded in molar ellipticity [Θ] ([Θ] = 3298Δϵ). *Mass spectra* were (ion-spray MS) recorded with an API-111 triple-quadrupole mass spectrometer (PE/sciex). The pneumatically assisted electrospray[21] (ion-spray)[22] interface was tuned at 0.5 kV. Following the evaporization of the solvent,[23] the ions were directed to the analyzer, where they experienced a potential difference of 0−120 V. After the separation due to the *m*/*z* ratio, they were detected by the electron multiplier with mass resolutions of 0.5 or 0.1 Da.

Multifrequency (Q-band, ∼34 GHz; X-band, ∼9.2 GHz, S-band, ∼4 GHz) EPR spectra, recorded as the first derivative of absorption, were obtained using a Bruker ESP300E EPR spectrometer. Cylindrical TE_{011} cavities, rectangular TE_{102} cavities, and a flexline resonator were used to measure the Q-, X-, and S-band EPR spectra, respectively.

(21) Yamashita, M.; Fenn, J. B. *J. Phys. Chem.* **1984**, *88*, 4451.
(22) Bruins, A. P.; Covey, T. R.; Henion, J. D. *Anal. Chem.* **1987**, *59*, 2642.
(23) Iribarne, J. V.; Thomson, B. A.; *J. Chem. Phys.* **1976**, *64*, 2287.
(24) Two different fractions of a white powder were isolated in independent reactions. Both have identical MS (ion-spray), UV−vis, and CD spectra but significant differences in the ^{1}H NMR spectra. Unambiguous reasons for these differences have not been identified so far, but all experiments reported here (spectroscopic analyses of the peptide, complexation with copper(II), and spectroscopic analyses of the mono- and dinuclear copper(II) compounds) have been done on a pure fraction of 22 mg of PatN that was combined from three independent cyclization/purification procedures.

Table 5. New MOMEC97 Atom Types and Nonbinding Parameters

atom type	mass	VdWr	ϵ	comment
SAH	32.06	2.00	0.185	S thiazole
CAH	12.01	1.90	0.044	C thiazole
NAH	14.01	1.80	0.050	N thiazole

Table 6. New Bond Stretch Parameters

bond type		k_r	r_0 [Å]	comment
CAH	CAH	1.300	1.370	thiazole
CAH	SAH	1.500	1.708	thiazole
ND	H	6.848	1.010	amide
ND	C	6.500	1.310	conj peptide
CON	CAH	7.400	1.520	peptide and Thz
CC	CT	5.113	1.504	amber
CU2P	ND	0.400	1.920	
CU2P	OW	0.800	1.900	ref 7 equatorial oxygen
CU2P	OP	0.100	2.500	ref 7 axial oxygen

Version 3.02 of Bruker's esp300e software was employed for data collection. A flow-through cryostat in conjunction with a Eurotherm (B-VT-2000) variable-temperature controller provided temperatures of 120−140 K at the sample position in the cavity. Calibration of the microwave frequency and the magnetic field were performed with an EIP 548B microwave frequency counter and a Bruker 035M gaussmeter.

Computer Simulation of EPR Spectra. Simulation of the mononuclear copper(II) EPR signal, measured as a function of magnetic field at a constant frequency, was performed using the simulation program Sophe[13] on a SUN SPARC Station 10/30. Determinations of the *g*- and hyperfine matrixes and the relative orientation of the two copper(II) sites from the EPR spectra of the dipole−dipole-coupled dinuclear copper(II) complexes were accomplished by simulating the $\Delta m_s = \pm 1$ resonances with the program DISSIM[18] on the SUN workstation. To date, the effect of *g*- and *A*-strain on the line widths has not been incorporated into this program. Consequently, the quality of the simulations is not expected to be as high as those for mononuclear copper(II) complexes; however, reproduction of the resonance field positions was attainable.

Molecular Dynamics Calculations. Structures were generated with the program CERIUS2 v.1.6 from Molecular Simulations, Inc., using the universal force field. Calculations were done with charges. The preoptimized structures were used as starting points for a search, based on a combination of structure optimization with three cycles of annealing dynamics, followed by a final optimization step. Annealed dynamics simulations were carried out at temperatures of 700−200 K, 500−200 K, and 400−200 K in 25 K increments and time steps of 1 fs with 50 steps per temperature increment. The lowest energy minimum structures were saved for subsequent optimization with molecular mechanics.

Molecular Mechanics Computations. MM computations were done with the modeling program MOMEC97,[19] using a previously published force field.[20] New parameters are listed in Tables 5−9.

Syntheses. Syntheses up to the linear octapeptide are available in the Supporting Information.

Cyclo(Ile-Ser-(Gly)Thz-Ile-Thr-(Gly)Thz) (PatN). HCl·Boc-Ile-Ser-(Gly)Thz-Ile-Thr-(Gly)Thz-OH (120 mg; 0.17 mmol) and HATU (190 mg; 0.51 mmol) were dissolved in 200 mL of dry DMF at room temperature. After the addition of DIPEA (0.29 mL; 215 mg; 1.7 mmol), the solution turned yellow. After being stirred for 1 h, the solution was acidified with HCl (5%) and turned a lighter shade of yellow. DMF was evaporated, and the crude product was purified with reverse-phase HPLC (gradient: water/0.1% TFA to 100% (10% water/90% acetonitrile/0.1% TFA) over 60 min). Analytical HPLC (gradient: water/0.1% TFA to 100% (10% water/90% acetonitrile/0.1% TFA) over 30 min): one peak, retention time 19 min. Yield: 20%. CD: λ_{max} [nm] = 274; $\Delta\epsilon$ [M^{-1} cm^{-1}] = +35. ISMS: *m*/*z* 695.2 $[M + H]^+$. HRMS (FAB+): *m*/*z* = 695.2652, $[M + H]^+$ calculated for $C_{29}H_{43}N_8O_8S_2$ 695.2566; *m*/*z* = 694.2548, M^+ calculated for $C_{29}H_{42}N_8O_8S_2$ 694.2566. ^{1}H NMR δ_H (d_4-MeOD, 400 MHz): 0.90, 0.91 (2t, 6H, 2 δ-CH_3-Ile, $^3J_{HH}$ = 7.4, 7.3 Hz); 0.99, 1.07 (2d, 6H, 2 γ-CH_3-Ile, $^3J_{HH}$ = 6.7, 6.8 Hz); 1.26 (d, 3H, CH_3-Thr, $^3J_{HH}$ = 6.6 Hz); 1.70, 1.80 (2m, 4H, 2

Table 7. New Valence Angle Parameters

angle type			k_0	θ_0 [rad]	comment
NAH	CAH	NAH	0.970	2.163	peptide−thiazole
CON	CAH	NAH	0.970	2.049	peptide−thiazole
CAH	CAH	CON	0.970	2.215	peptide−thiazole
ND	CON	CAH	0.250	2.067	peptide−thiazole
OCO	CON	CAH	0.250	2.067	peptide−thiazole
CT	CON	ND	0.250	2.180	
CAH	CT	ND	0.450	1.911	
CON	CT	ND	0.450	1.936	
CT	CT	OR	0.450	1.911	
OR	CT	H	0.360	1.909	
CON	ND	H	0.380	2.093	amber
CT	ND	H	0.380	2.140	amber
CT	ND	CON	0.250	2.140	amber
CT	OW	H	0.320	1.902	
CT	OW	CU2P	0.200	2.094	
SAH	CAH	CT	0.650	2.130	thiazole
SAH	CAH	H	0.350	2.094	thiazole
SAH	CAH	CAH	0.120	1.955	thiazole
CAH	SAH	CAH	0.300	1.570	thiazole
NAH	CAH	SAH	0.150	1.955	thiazole

Table 8. New Torsion Angle Parameters

bond	k_ϕ	m	ϕ [rad]	comment
** CAH CON **	0.0030	2.00	0.087	
** CAH CAH **	0.015	2.00	1.571	ref 7
** CAH CT **	0.0005	6.00	0.524	ref 7
** CAH NAH **	0.0090	2.00	1.571	ref 7
** CCO OP **	0.0045	2.00	0.524	ref 7
** CT NAH **	0.0005	6.00	0.524	ref 7
** OR CT **	0.0039	3.00	0.00	
** NAH NAH **	0.0200	2.00	1.571	ref 7
** SAH CAH **	0.0150	2.00	1.571	

Table 9. New Out-of-Plane Parameters

atom plane				k_δ	comment
CAH	CAH	SAH	H	2.00	thiazole
CAH	SAH	NAH	CT	2.00	thiazole
CT	H	H	H	0.00	
CT	CAH	H	H	0.00	thiazole
CAH	CAH	CAH	H	2.00	thiazole
CAH	CAH	NAH	CT	2.00	thiazole
CAH	CAH	NAH	H	2.00	thiazole
CAH	CON	NAH	CAH	2.00	thiazole
CON	ND	OCO	CAH	2.00	
NAH	CU2P	CAH	CAH	0.00	thiazole

γ-CH_2-Ile); 2.40, 2.50 (2m, 2H, 2 β-C*H*-Ile); 3.89 (d of d, 1H, β-CH_2-Ser, $^3J_{HH}$ = 3.5 Hz, $^2J_{HH}$ = 11.3 Hz); 3.97 (d, 1H, α-C*H*-Thr); 3.98 (d of d, 1H, β-CH_2-Ser); 4.15, 4.19 (2d, 2H, 2 α-C*H*-Ile, $^3J_{HH}$ = 3.12, 3.0 Hz); 4.30, 4.31 (2d, 2H, CH_2-Gly, $^2J_{HH}$ = 17.3, 17.2 Hz); 4.474 (d of d, 1H, α-C*H*-Ser, $^3J_{HH}$ = 5.4, 5.3 Hz); 4.641 (d of q, 1H, β-C*H*-Thr, $^3J_{HH}$ = 3.7, 6.5 Hz); 5.14, 5.20 (2d, 2H, CH_2-Gly, $^2J_{HH}$ = 17.2, 17.3 Hz); 7.58, 7.60 (2s, 2H, 2 C*H*-Thz); 8.15, 8.25 (2 d of d, 2H, 2 N*H*-Gly); 8.92 (d, 1H, N*H*-Ser); 9.15, 9.50 (2d, 2H, 2 N*H*-Ile); 9.60 (d, 1H, N*H*-Thr). Chemical shift data and assignments are compiled in Table 1.

Peptide Content of PatN. Because PatN is hygroscopic and residual amounts of TFA may be present after purification with reverse-phase HPLC, the peptide content needed to be determined to avoid the addition of excesses of copper(II) salts. PatN (2 mg) was dissolved in methanol, and enough triethylamine was added to deprotonate the amides. Subsequently, this solution was titrated with a standard stock solution of $CuCl_2$ in methanol while being monitored with UV−vis spectroscopy. The titration came to an end when a plateau region was reached at the addition of 2 equiv of copper (absorption intensity remains the same). Using the amount of copper(II) salt solution added, it was calculated that the peptide content was 78%. To positively avoid a copper(II) salt excess, the following syntheses were done assuming a peptide content of 75%. It should be emphasized that all of the following experiments involving PatN were performed with milligram quantities of PatN, as only limited quantities were synthesized.

Mononuclear Copper(II) Complexes. To 2 mL of a 0.002 M solution of PatN in methanol was added 1 equiv of a 0.022 M solution of $Cu(NO_3)_2$ in methanol. To this mixture was added 1−2 equiv of a 0.05 M solution of triethylamine in methanol, dropwise, and the resulting solution was stirred after each addition. MS (addition of 2 equiv base): $[PatNH_7]^+$ m/z = 695.4 (calc 695.5), rel int 100%; $[PatN(NEt_3H)]^+$ m/z = 796.4 (calc 796.6), rel int 80%; $[Cu(PatNH_5)]^+$ m/z = 756.0 (calc 757.0), rel int 83%; $[Cu_2(PatNH_6)(OH)_3]^+$ m/z = 872.1 (calc 872.6), rel int 34%; $[Cu_2(PatNH_6)(H_2O)_2Cl]^{3+}$ m/z = 299.0 (calc 297.7), rel int 85%; $[Cu_2(PatNH_6)(NEt_3H)(OH)_2]^{3+}$ m/z = 318.2 (calc 319.2), rel int 91%. UV−vis λ_{max} [nm] (ϵ [M^{-1} cm^{-1}]): addition of 1 equiv base 220 (30 000), 708 (43); addition of 2 equiv base 220 (30 000), 585 (91). CD λ_{max} [nm] ($\Delta\epsilon$ [M^{-1} cm^{-1}]): addition of 1 equiv base 263 (+8.3), 600 (−0.45); addition of 2 equiv base 270 (+5.97) 590 (−1.36). EPR data are compiled in Table 2.

Dinuclear Copper(II) Complexes. To 2 mL of a 0.002 M solution of PatN in methanol was added 2 equiv of a 0.022 M solution of $Cu(NO_3)_2$ in methanol. Four (blue complex) to 5 (purple complex) equiv of a 0.0125 M solution of NaOH in methanol was added dropwise, and the solution was stirred after each addition. MS (addition of 4 equiv base): $[PatNH_7]^+$ m/z = 695.0 (calc 695.5), rel int 98%; $[PatN(NEt_3H)]^+$ m/z = 796.2 (calc 796.6), rel int 80%; $[Cu_2(PatNH_6)(OH)_3]^+$ m/z = 872.3 (calc 872.6), rel int 25%; $[Cu_2(PatNH_6)(H_2O)_2Cl]^{3+}$ m/z = 299.0 (calc 297.7), rel int 74%; $[Cu_2(PatNH_6)(NEt_3H)(OH)_2]^{3+}$ m/z = 318.2 (calc 319.2), rel int 100%. MS (addition of 5 equiv base): $[PatNH_7]^+$ m/z = 695.0 (calc 695.5), rel int 95%; $[(PatNH_6)Na]^+$ m/z = 717.2 (calc 717.5), rel int 67%; $[PatN(NEt_3H)]^+$ m/z = 795.8 (calc 796.6), rel int 62%; $[Cu_2(PatNH_6)(OH)_3]^+$ m/z = 872.3 (calc 872.6), rel int 25%; $[Cu_2(PatNH_4)Na]^{3+}$ m/z = 280.9 (calc 280.9), rel int 88%; $[Cu_2(PatNH_6)(H_2O)_2Cl]^{3+}$ m/z = 298.6 (calc 297.7), rel int 81%; $[Cu_2(PatNH_6)(NEt_3H)(OH)_2]^{3+}$ m/z = 318.4 (calc 319.2), rel int 100%. MS (negative ions): $[Cu_2(PatNH_4)(OH)_3(Cl)(Na)]^-$ m/z = 929.0 (calc 929.0), rel int 32%; $[Cu_2(PatNH)]^-$ m/z = 817.0 (calc 816.6), rel int 36%; $[Cu(PatNH_3)]^-$ m/z = 756.0 (calc 755.0), rel int 17%; $[Cu_2(PatNH_4)(NO_3)(OH)_3]^{2-}$ m/z = 465.0 (calc 466.3), rel int 67%; $[Cu_2(PatN)]^{2-}$ m/z = 407.7 (calc 407.8), rel int 65%; $[Cu_2(PatNH_2)(OH)_3]^{3-}$ m/z = 289.5 (calc 289.5), rel int 100%. UV−vis λ_{max} [nm] (ϵ [M^{-1} cm^{-1}]): addition of 4 equiv base 220 (30 000), 364 (900), 590 (140); addition of 1 equiv base 220 (30 000), 367 (10 580), 540 (210). CD λ_{max} [nm] ($\Delta\epsilon$ [M^{-1} cm^{-1}]): addition of 4 equiv base 340 (+22.70), 496 (+3.94), 600 (−13.64); addition of 5 equiv base 335 (+6.67), 372 (−1.73), 490 (2.24), 590 (−12.13). EPR data are compiled in Table 3.

Acknowledgment. Generous financial support by the German Science Foundation (DFG) and the Fonds of the Chemical Industry (FCI) is gratefully acknowledged. This project has also been supported by a DAAD/ARC grant.

Supporting Information Available: Preparative details and analytical data for all intermediates up to the linear octapeptide and plots of the UV−vis titrations and of Q-, S-, and X-band EPR spectra (experimental and simulations) (13 pages). Ordering information is given on any current masthead page.

IC9809299